The 7th International Supercritical CO_2 Power Cycles Symposium
March 31 – April 2, 2020, San Antonio, Texas
Paper #60

Magnetic Journal Bearing Instability Under Supercritical CO_2 Conditions

Dokyu Kim
Master Student
Korea Advanced Institute of Science and Technology
Daejeon, Korea

Jeong Ik Lee
Professor
Korea Advanced Institute of Science and Technology
Daejeon, Korea

SeungJoon Baik

Korea Atomic Energy Research Institute
Daejeon, Korea

ABSTRACT

Because reducing the CO_2 emission is imperative, supercritical CO_2 (S-CO_2) power cycle is developed with its improved power generation efficiency power density. However, to commercialize this cycle, hermetic bearing technology is essential. To sustain S-CO_2 power cycle's compactness, hermetic bearing is better than oil lubrication system because it requires additional oil supply or sealing/suction system. Among the hermetic bearing types, magnetic bearing can be a good option with large load capacity. However, from several studies on the magnetic bearing, the instability issues with S-CO_2 working fluid and high speed operating conditions were repeatedly mentioned. This issue was related to the fluid conditions, mostly pressure and density. Because of this issue, the magnetic bearing sometimes cannot maintain enough clearance for the rotor leading to physical contact and consequently damaging the system. Thus, this issue should be thoroughly studied and be resolved for the successful and steady operation of the power system. The instability by fluid force exerted on the rotating shaft can be modeled with the Reynolds equation. For the first step, the steady lubrication analysis model is developed. The model calculation results imply that the lubrication performance is quite sensitive to the CO_2 condition especially density gradient. Based on this finding, an experimental system is designed to investigate this issue. Therefore, designed facility can control the fluid conditions. To study the instability issues experimentally, an impeller of the test compressor is removed to make the main instability factor as the interaction between the rotor and the bearing only through the working fluid. The shaft position and the electric current data are collected from the magnetic bearing controller. From the data, the lubrication force can be separated from the net force. These results are compared with the analytical lubrication model. By adding the transient term and heat balance model, it will be possible to define the unstable operating conditions and suggest the required magnetic bearing performance for S-CO_2 conditions.

INTRODUCTION

Interests in the S-CO_2 power cycle technology are growing due to its many advantages. An S-CO_2 Brayton cycle has high efficiency (~50%) with moderate temperature heat sources (450~750°C) [1]. It also has compact component and simple configuration. These advantages mainly originate from the S-CO_2 thermal fluid properties like high density, low expansion rate, no phase change above critical point and high recuperation rate. These characteristics of S-CO_2 cycle make possible to realize distributed power generation.

However, in order to commercialize the S-CO_2 Brayton power cycle for the distributed power generation market, developing an appropriate bearing technology for the power cycle has been identified as the major challenge among many technical issues. Due to the rotating motion of the turbomachinery, bearings are necessary to support the rotating shaft in all directions. In this manner, designing a high speed S-CO_2 turbomachinery with reliable bearing system has always been emphasized for the development of the S-CO_2 power cycle. A bearing system should be properly selected as the power of an S-CO_2 cycle shown in Figure 1. The gas foil bearing technology becomes very challenging to support a shaft for the turbomachinery for 3MWe or higher power output system. For various applications, improving bearing performance is required. Hydrodynamic oil bearing and hydrostatic bearing can bear larger load than other bearing technologies. However, because most of oils dissolve well in S-CO_2 condition, maintaining the S-CO_2's purity without complex system is problematic for the long-term reliable operation of the cycle [2], [3]. Thus, the magnetic bearing technology can be very favorable option for the S-CO_2 cycle commercialization.

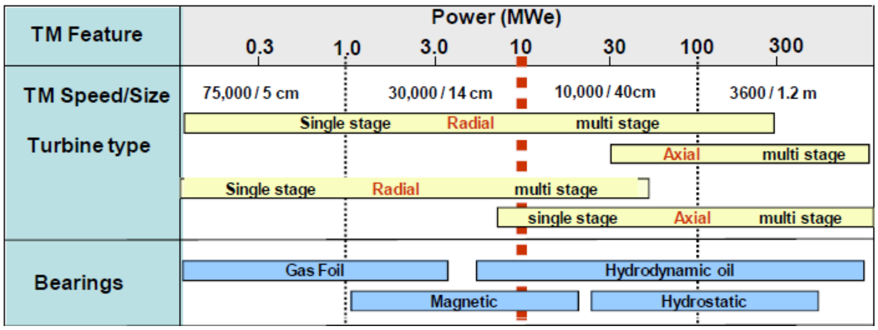

FIGURE 1. Bearing options for S-CO_2 Brayton cycles with various power scales [4]

There were several experiments related to the magnetic bearing for an S-CO_2 power cycle. However, from these experiments, magnetic bearing operation under S-CO_2 power cycle condition was not reported to be successful. These studies repeatedly mention the instability issue from high speed operation test under high pressure S-CO_2 conditions. An example experimental result proceeded by KAERI and KAIST is shown in Figure 2. The shaft position data is not given because the experiments are operated with only shaft monitoring program.

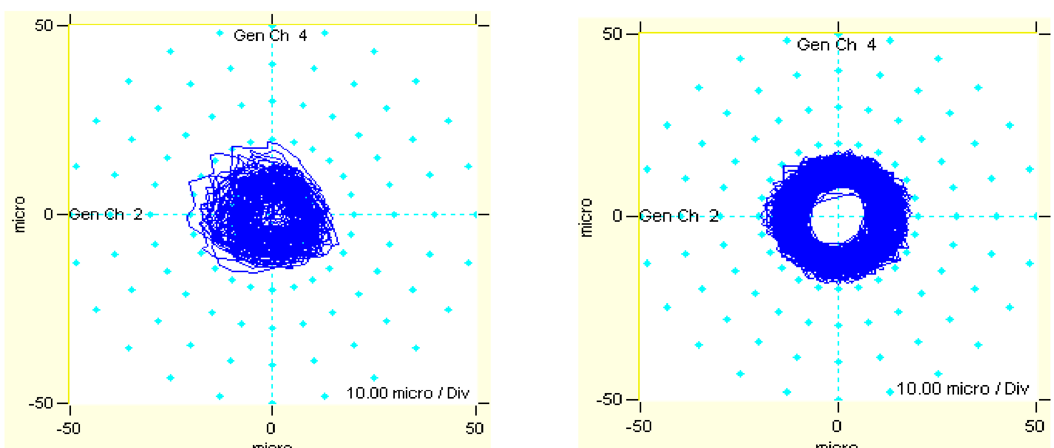

FIGURE 2. Shaft motion with magnetic bearing control under S-CO_2 condition (left, 14000 RPM, 43.42 ℃ & 78bar) and atmospheric condition (right, 30000 RPM) from KAERI

Since the instability induces the shaft eccentricity to grow until the clearance between shaft and stator disappears leading to contact, the rotational speed could not be increased during the test. In contrast, higher speed operation was possible for normal air condition and the shaft seems stable in this test. Since the magnetic bearing also has working fluid in the clearance between the shaft and the bearing, it can be concluded that the instability issue was related to the fluid conditions in which the bearing is operating such as pressure and density. Therefore, the instability issue will be viewed from the perspective of thin film lubrication model in this paper first to develop a simple model for analyzing the interaction between S-CO_2 lubricating fluid and bearing shaft. In this paper, the developed S-CO_2 lubrication model is introduced. From the discussion of the developed model results, the instability source of the magnetic bearing operation is predicted and the magnetic bearing experimental process is designed. The experiment focuses on the verification of this model and finding the cause of instability and a method to resolve it.

RESULTS AND DISCUSSION

Characteristics of active control magnetic bearing

Active-control Magnetic Bearing (AMB) levitates the rotating shaft with electromagnets around the shaft. Therefore, no lubricant is required. The number of electromagnets are not fixed but usually 8 symmetrically located type is used as shown in Figure 3 [5].

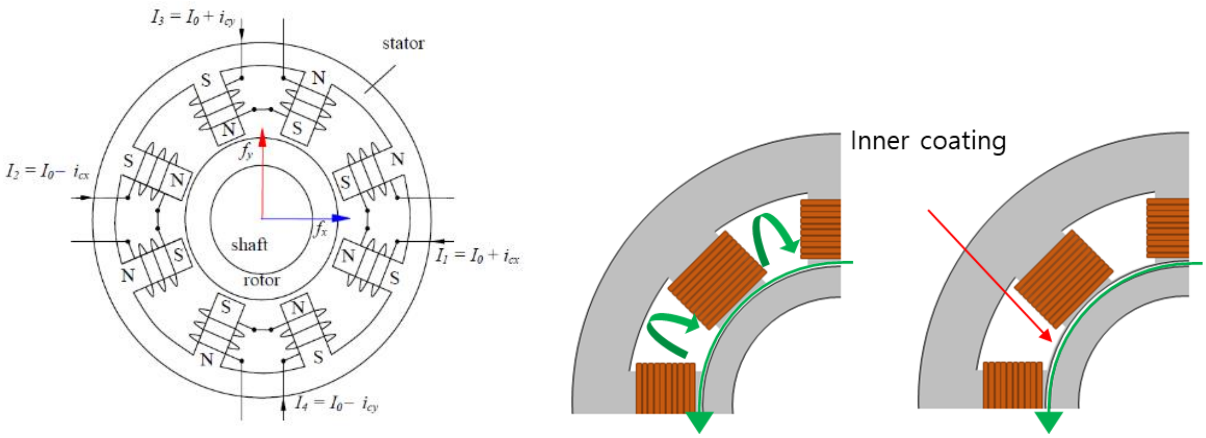

FIGURE 3. Magnetic bearing description (Electromagnets in the magnetic bearing [5] and inner fluid effects without shielding)

The empty space between the shaft and the bearing is filled with the working fluid, which flows through the labyrinth seal. Therefore, the spaces between the electromagnets can generate unwanted vortices and affect the shaft motion. This situation is depicted in Figure 3.

Lubrication analysis model for the S-CO_2 fluid

To obtain the force applied to the shaft from the lubrication effect of fluid, the pressure distribution around the shaft should be first calculated. Reynolds equation can be used for the analysis model [6]. This equation is a partial differential equation for a thin film flow. Reynolds equation for lubrication is derived by substitution of the velocity profile from Navier-Stokes equation to the continuity equation. With turbulent model which is described in table 1 and ignoring axial direction, the equation can be written as below.

$$\frac{\partial}{\partial X}\left(\frac{\rho h^3}{k_x \mu}\frac{\partial p}{\partial X}\right) = \frac{1}{2}\frac{\partial(\rho h u)}{\partial X} + \frac{\partial(\rho h)}{\partial t}, \qquad k_x = 12 + K_x Re^{n_x} \quad (1)$$

Table 1 Coefficient in Ng-Pan model [7]

Reynolds' number	K_x	n_x
50,000<Re	0.0388	0.8
5000<Re<50000	0.0250	0.84
Re<5000	0.0039	1.06

Before using equation (1), the coordinate system of the bearing has to be determined as shown in Figure 4. Furthermore, the shaft position and motion with this coordinate system should be given. The shaft position is given with the biased length, e. The shaft motion is assumed to be revolving with the same frequency of rotation and radius e. With these assumptions, the pressure distribution around the shaft with inner-coated magnetic bearing can be calculated from solving the equation (1).

The governing equation is numerically solved with the Finite Difference Method (FDM). The coordinate and thin film geometry for the FDM is described in Figure 4. To solve the FDM, spatially uniform initial thermal properties are substituted into the equation (1). These values can be obtained from the supply temperature and pressure. Then, the pressure distribution can be obtained by iterative calculation by updating the thermal properties with calculated pressure distribution. This process is described in the flow chart as shown in Figure 5 and implemented with MATLAB code.

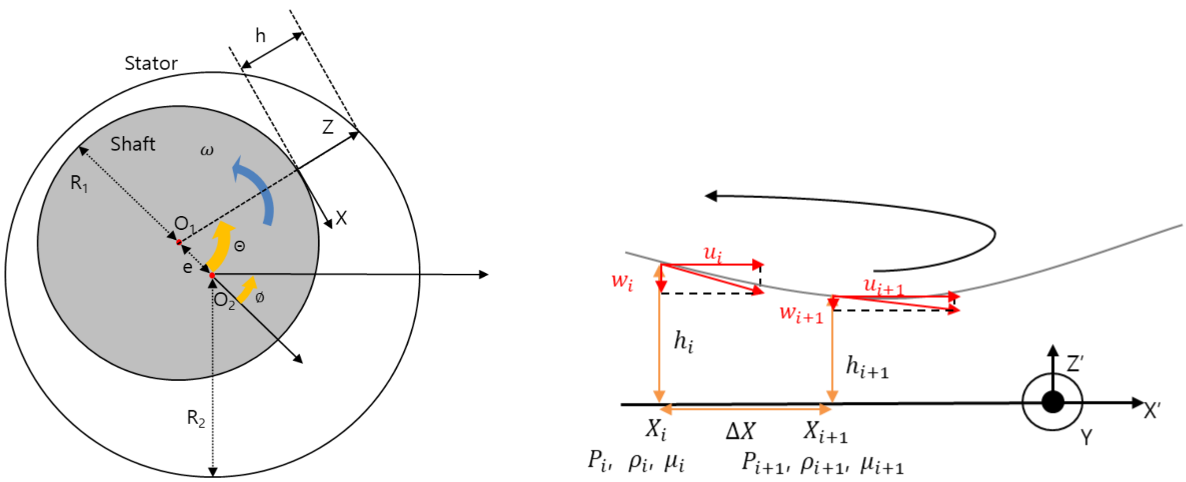

FIGURE 4. Geometry of the lubrication system with unbalanced shaft (left) and the FDM geometry (right)

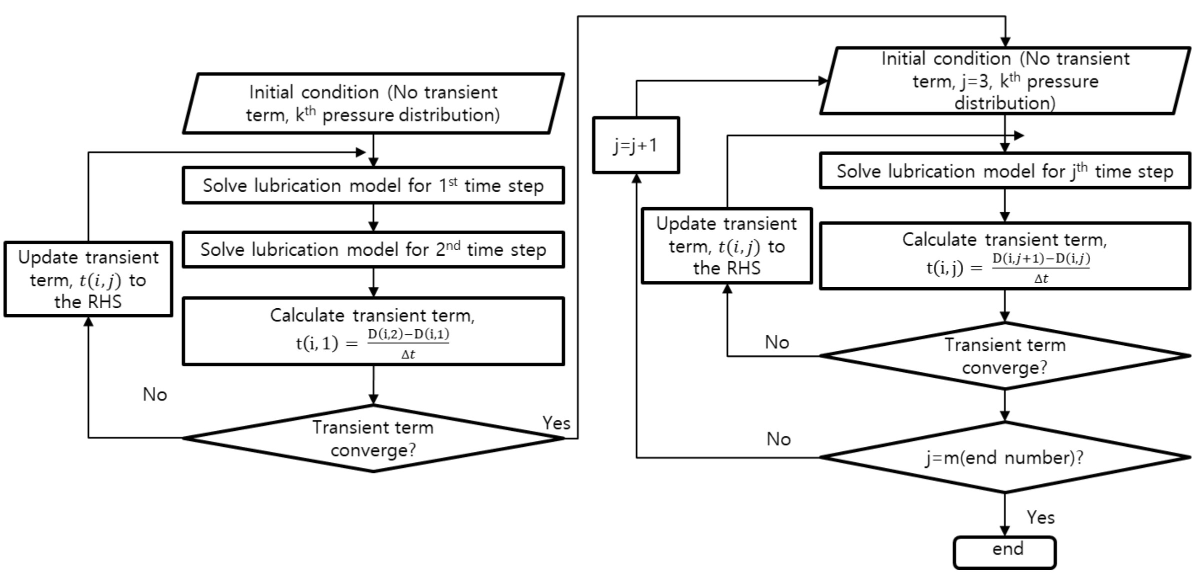

FIGURE 5. Flow chart of the pressure calculation

Analysis of the pressure distribution from the turbulent lubrication model results

The analysis range is defined and unstable operating conditions were searched. The inlet pressure range is from 70bar to 100 bar. This is for the comparison between the high speed operation in air condition and the CO_2 condition with 1bar so the effect of the pressure and the fluid type, density can be compared. The temperature is near the CO_2's critical temperature which is also close to the room temperature. The rotational speed is 30,000 RPM. The rotation condition is defined as in Figure 6 for convenience so the shaft is biased to the left only. The eccentricity ratio, ε is the ratio between the eccentricity, e, and the nominal clearance, c = $R_2 - R_1$. ε' s upper limit is given as 0.1 as reflecting the former experiment. The calculation results from the model is important for designing the magnetic bearing experiment. From the developed model, the pressure distributions for various conditions are obtained as shown in Figure 6. They also show that the distributions become wider as the eccentricity increases.

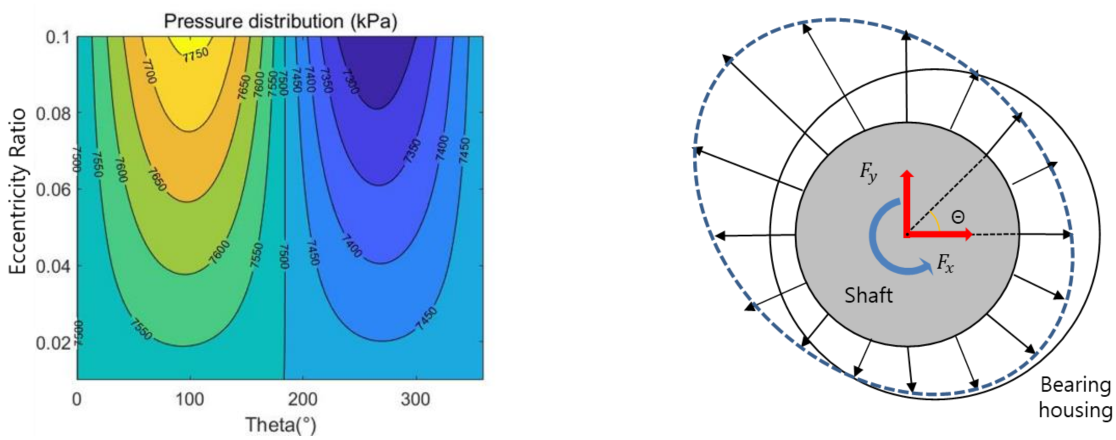

FIGURE 6. Pressure distribution around rotating shaft (7.5 MPa, 30 ℃ CO_2)

Force analysis under various thermal condition

The relationships between the force exerted on the shaft and the thermal conditions of the CO_2 are analyzed as shown in Figure 6. The $\boldsymbol{F_x}$ and the $\boldsymbol{F_y}$ in Figure 6 under various thermal conditions of CO_2 have shown that the fluid conditions influence the shaft motion. $\boldsymbol{F_x}$ and $\boldsymbol{F_y}$ for 30,000 RPM are shown in Figure 7. This figure shows that $\boldsymbol{F_x}$ is applied in the opposite direction of the eccentricity and its peak point is distributed near CO_2's pseudocritical line. $\boldsymbol{F_y}$ is mostly applied to the downward direction but upward direction for near critical point. Also, it increases as the temperature of the CO_2 decreases or the pressure increases. It is assumed to be mainly proportional to the density.

From these results, it is concluded that the attitude angle where the net forces will be opposite direction of the gravity will usually have a value between 1.5π to 2π but this angle would be drastically changed near critical point as the $\boldsymbol{F_y}$'s direction becomes opposite. This is observed as Figure 8. The forces' rapid change near the pseudo-critical line from the rapid density change is assumed to be not shown for air bearing case so these characteristics could be the cause of the instability. In addition, because of the high sensitivity of these forces to the thermal properties, heat transfer analysis is required to have better accuracy of the model. This is planned to be done by modifying the lubrication model, CFD analysis and experiments. To analyze the cause of the $\boldsymbol{F_x}$'s rapid change near the critical point, additional calculations are performed with the developed lubrication model.

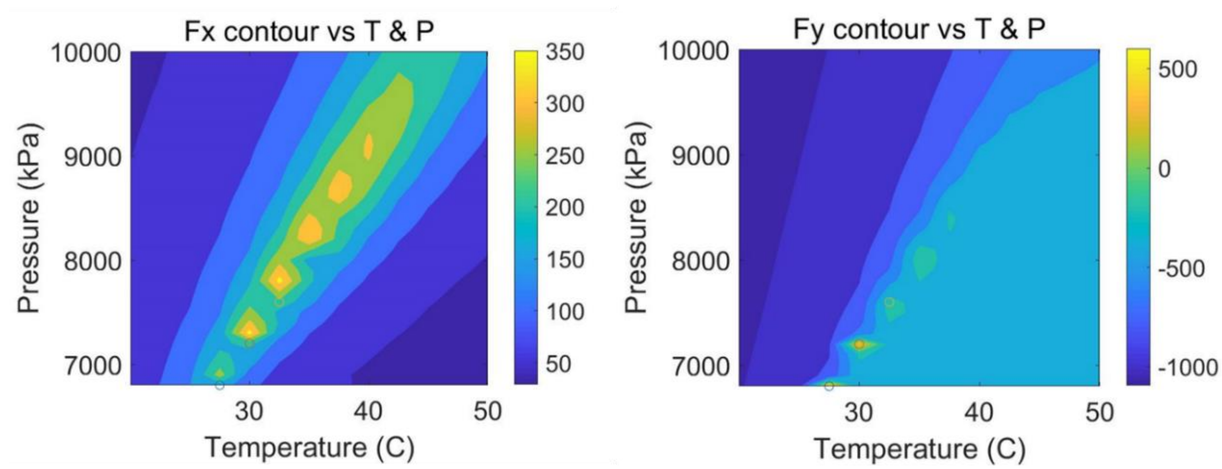

FIGURE 7. $\boldsymbol{F_x}$ **(left) and** $\boldsymbol{F_y}$ **(right) for various conditions (30,000 RPM)**

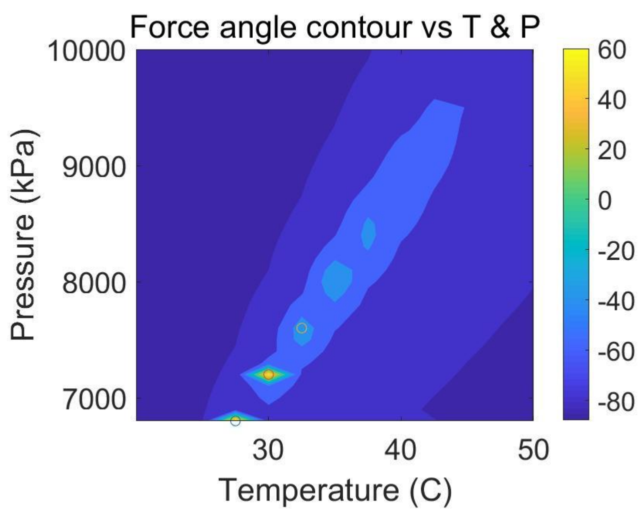

FIGURE 8. Lubrication force angle for various conditions (30,000 RPM)

For the comparison, high density and the same pressure air is also evaluated with the developed model. To find the main reason of the difference between air and CO_2 condition, the term $\frac{1}{2}\frac{\partial(\rho h u)}{\partial X}$ in the equation (1) is separated as $\left(\frac{hu}{2}\right)\frac{\partial\rho}{\partial X}+\left(\frac{u}{2}\frac{\partial h}{\partial X}\right)\rho$. The terms of the RHS around the shaft is plotted in Figure 9 and it is concluded that the significant difference is generated from the density's spatial and temporal change around the shaft. The forces calculated from this is organized as Table 2 and it is concluded that the density changes induce $\boldsymbol{F_x}$ to become larger.

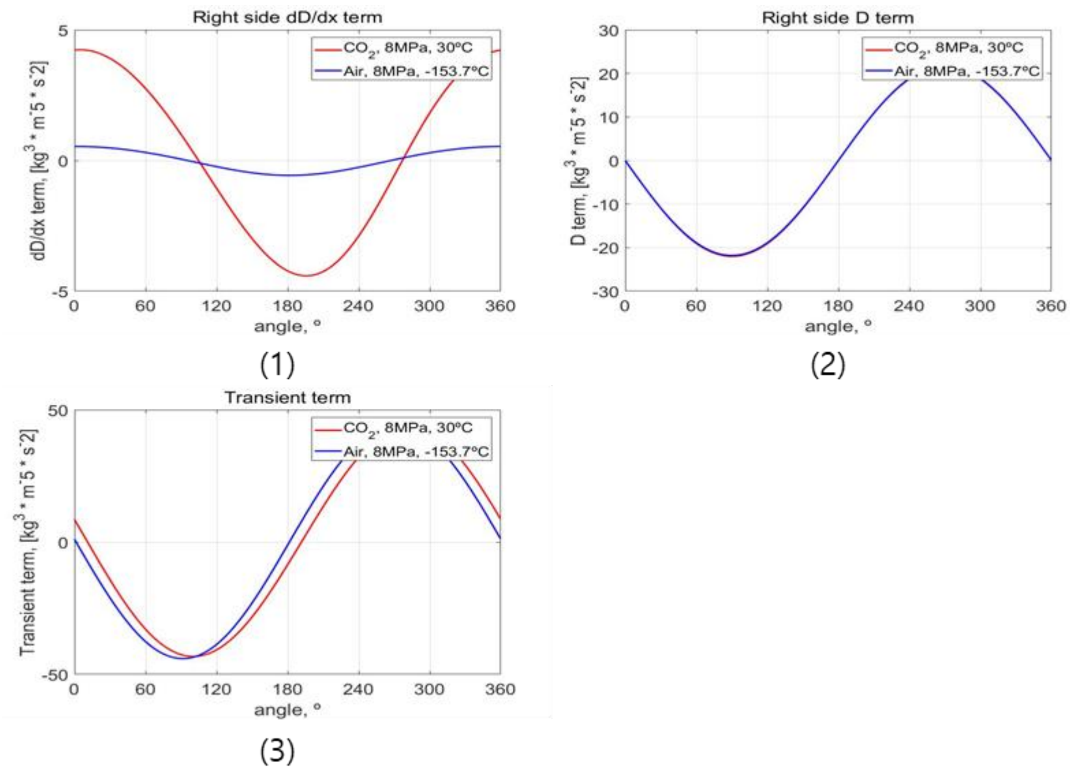

FIGURE 9. $\left(\frac{hu}{2}\right)\frac{\partial\rho}{\partial X}$ **(1),** $\left(\frac{u}{2}\frac{\partial h}{\partial X}\right)\rho$ **(2) and** $\frac{\partial(\rho h)}{\partial t}$ **(3) term around the shaft for various thermal conditions (ε= 0.08 and 30,000 RPM)**

Table 2. Forces on the shaft for various thermal conditions and ε = 0.25 and 30,000 RPM

Thermal condition	F_x (N)	F_y (N)
Air at 8 MPa, -153.7 ℃	35.3	-1433.6
CO_2 at 8 MPa, 30 ℃	265.2	-1344.7

Experimental study of the lubrication effects on magnetic bearing

The objectives of the magnetic bearing test are analyzing the instability and determining the required magnetic bearing performance to successfully support the shaft. The control logic or the design of the magnetic bearing can be modified with an improved modeling from the magnetic bearing test. In addition, the lubrication model can be modified based on the test results.

Based on the lubrication modeling results, it was concluded that the experimental facility should be able to handle various thermal conditions of fluid. Therefore, preexisting S-CO_2 pressurizing experiment (S-CO_2PE) facility is utilized for creating appropriate testing conditions. S-CO_2PE consists of an S-CO_2 pump, a Printed Circuit Heat Exchanger(PCHE) type pre-cooler and water cooling loop so the temperature and the pressure can be controlled. This facility is shown in Figure 10.

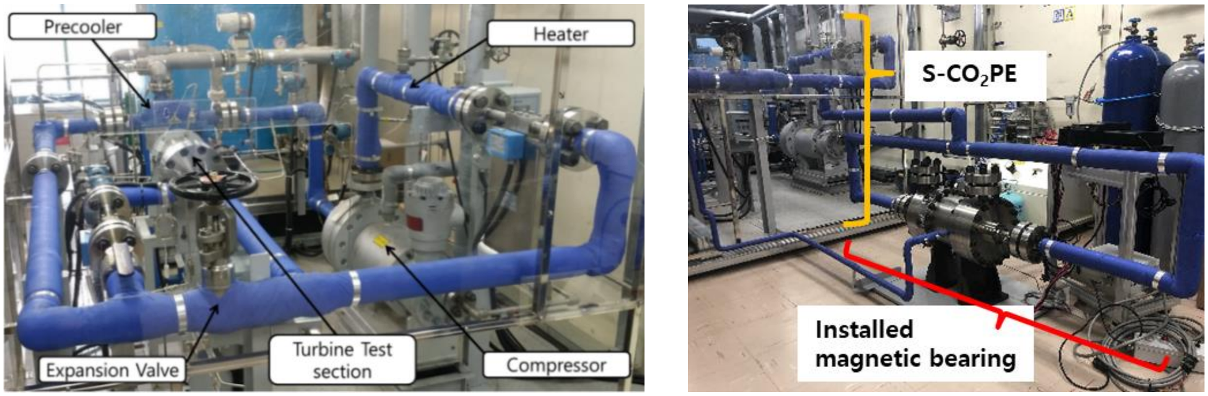

FIGURE 10. S-CO_2 power cycle demonstration facility (S-CO2PE, left) and magnetic bearing & compressor system (right)

The magnetic bearing test rig is manufactured to verify the developed model as shown in Figure 11. It shows that the test rig consists of the compressor mock up, the magnetic bearing and its controller. The impeller part is removed to analyze the sole effect of the thin film phenomena surrounding the rotating shaft. To obtain the experimental data, the signal from the displacement sensor is used for active control and the electric current flowing into the electromagnets are measured and calibrated for the magnetic force measurement.

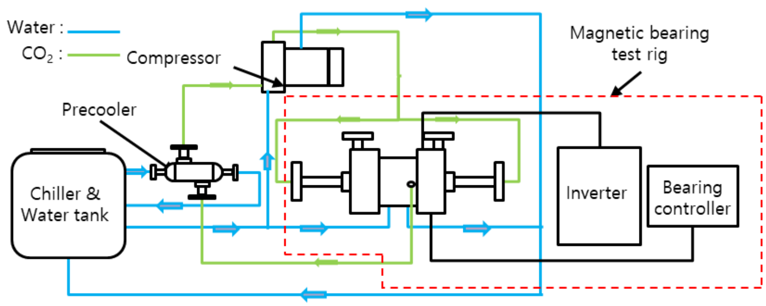

FIGURE 11. Layout of the magnetic bearing instability experiment

Analysis of magnetic bearing test

S-CO_2 tests were performed under 30,000 RPM and 9 MPa & 50 ℃, (290kg/m^3). From the shaft trajectory data as shown in Figure 12, it is observed that the shaft motion does not keep single revolving center. This position data with S-CO_2 test is compared with vacuum test by Fast Fourier Transform (FFT) as shown in Figures 13 and 14.

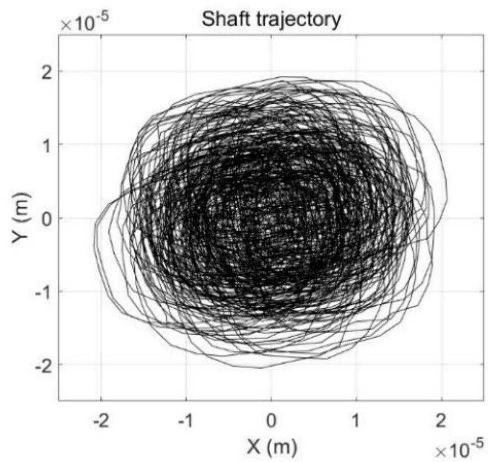

FIGURE 12. Shaft trajectory data

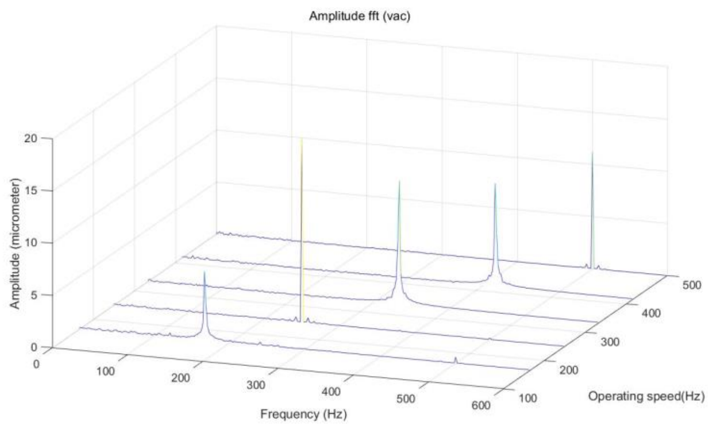

FIGURE 13. Fourier transform of the shaft trajectory data from vacuum test

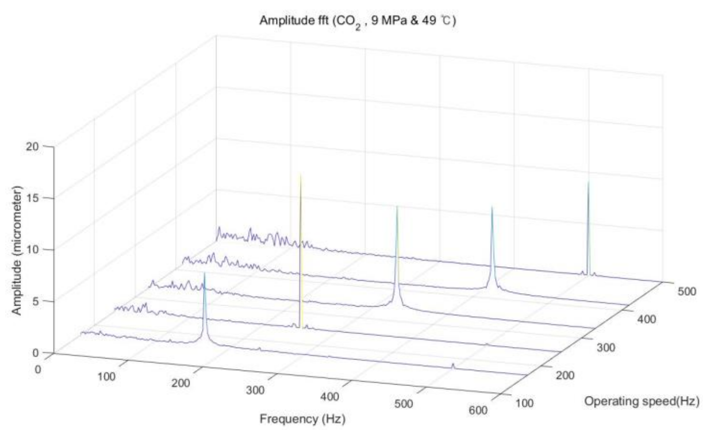

FIGURE 14. Fourier transform of the shaft trajectory data from S-CO_2 test

By comparing the Figure 13 and 14, specific noise is appeared in low frequency range in S-CO_2 test where usually is lubrication instability region but there is no clear peak for lubrication whirl or whip. The reason is assumed that the operation speed is not enough. The reason of the noise is assumed to be the S-CO_2's rapid density change. This noise can enhance the whip or whirl.

The given shaft trajectory data is also used as an input of the developed lubrication model.

The results of it is obtained with force on the shaft. The force is fitted with the eccentricity in Figure 17's left one and fitted with not only the eccentricity but also the transient term in Figure 15's right one. By comparing those two figures, it is concluded that the lubrication force's dispersion with eccentricity is occurred by the density change.

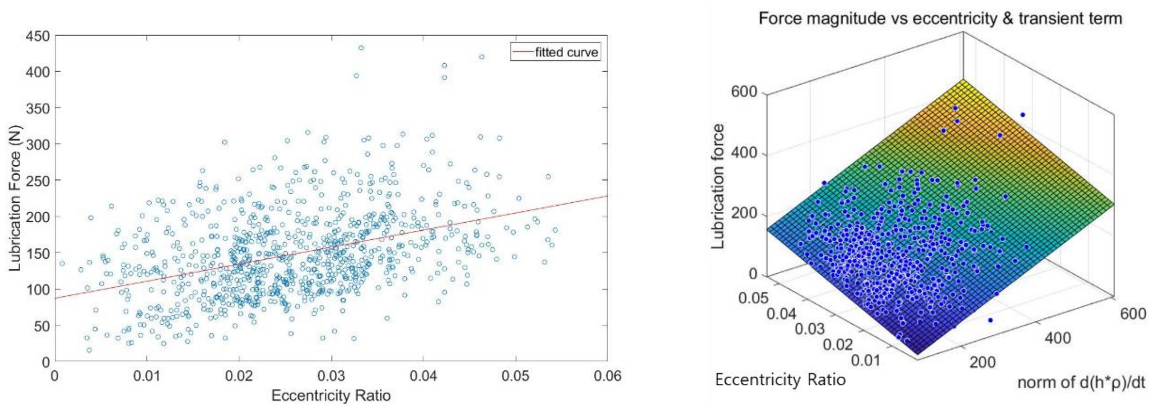

FIGURE 15. Linear fitting of the force with eccentricity and the density change

The stiffness of the CO_2 lubricant under 30,000 RPM and 9 MPa & 50 ℃, (290kg/m^3) condition is calculated as 6.4675 $\mathrm{N/\mu m}$ but they are affected by the shaft's motion. The vibration coefficients (stiffness, damping coefficient) will be further obtained precisely and presented in the symposium. Experiments with various thermal conditions are planned to find the relationship between these coefficients and the fluid thermal conditions.

The spaces between the electromagnets can generate vortex flow which can destabilize the shaft. So an additional magnetic bearing test is planned to by filling the gap with inner-coating to remove this geometry complexity. As described in Figure 3, this modification will create ideal environment to apply the Reynolds equation for the bearing analysis by removing geometrical uncertainties. Also, the heat transfer model will be added to analyze the effect of the temperature distribution around the shaft.

Summary and further works

From the lubrication model, it is concluded that the thermal property can affect the magnetic bearing control. Based on this result, an experimental system is designed and constructed to test hypothesis. An experiment was performed for verifying the model and check the instability sources. By utilizing the measured data and the model was further refined but still the model and data have discrepancy. This difference is thought to be caused by the non-ideal geometry of the electromagnets and non-uniform temperature distribution in the gap. Therefore, the model will be further developed to incorporate this effect as well as modifying the test section to have ideal geometry condition.

The test with gap-filled magnetic bearing is planned to commence in the near future. From this test, it is expected that the lubrication effects with close to ideal geometry can be finally compared fairly. By implementing these processes, the unstable operating region will be defined and the required performance of the magnetic bearing will be determined. From the modified model, dynamics of the shaft will be established for several different conditions. The trajectory of the shaft can be obtained from data and can be compared to the transient analysis of the rotor. If the model is well validated, this model can be utilized in various S-CO_2 cycle systems. After developing an accurate model, the control logic of the magnetic bearing can be finally suggested.

REFERENCES

[1] V. Dostal et al., ‘A Supercritical Carbon Dioxide Cycle for Next Generation Nuclear Reactors’, MIT-ANP-TR-100, 2004.

[2] Tsuji, Tomoya, et al. "Solubility and Liquid Density Measurement for CO2+ Lubricant at High Pressures." *Asian Pacific Confederation of Chemical Engineering congress program and abstracts Asian Pacific Confederation of Chemical Engineers congress program and abstracts*. The Society of Chemical Engineers, Japan, 2004.

[3] Seeton, Christopher J., and Predrag Hrnjak. "Thermophysical properties of CO2-lubricant mixtures and their affect on 2-phase flow in small channels (less than 1mm)." (2006).

[4] Sienicki, James J., et al. "Scale dependencies of supercritical carbon dioxide Brayton cycle technologies and the optimal size for a next-step supercritical CO2 cycle demonstration." *SCO2 power cycle symposium*. 2011.

[5] Shelke, Santosh. "Controllability of Radial Magnetic Bearing." *Procedia Technology* 23 (2016): 106-113.

[6] Hamrock, Bernard J., Steven R. Schmid, and Bo O. Jacobson. *Fundamentals of fluid film lubrication*. CRC press, 2004.

[7] Taylor, C. M., and D. Dowson. "Turbulent lubrication theory—application to design." *Journal of Lubrication Technology* 96.1 (1974): 36-46.